The Corrosion at 600°C of Four 8-12 Wt% Cr Ferritic Steels in Chemically Cycling Oxidizing-Sulfidizing Gases Starting With Sulfidation

F. Gesmundo°, C. Roos°, D. Oquab* and F. Viani°

°*Istituto di Chimica, Facoltà di Ingegneria, Università di Genova, Fiera del Mare, Pad. D, 16125 Genova, Italy*

**Laboratoire des Matériaux, Ecole Nationale Superieure de Chimie, 118 Route de Narbonne, 31077 Toulouse, France*

(Received September 24, 1997)

ABSTRACT

The corrosion of four ferritic steels containing 8-12 wt% Cr was studied at 600°C in gas mixtures whose composition changed cyclically with time from sulfidizing to oxidizing conditions and vice versa. The initial cycle was sulfidizing, while each cycle lasted 24 hr and the maximum number of cycles was four. Oxidation after the first sulfidizing cycle produced a layer of iron oxides growing over the initial sulfide layer at rates much higher than for the pure oxidation of the same materials at the same temperature. The second sulfidizing stage produced thin sulfide scales over the oxide layer, growing much more slowly than during the initial sulfidation. Finally, the second oxidizing stage produced porous external oxide layers growing mainly directly in contact with those formed during the first oxidizing stage, while the second sulfide layer tended to disappear. The corrosion behavior of the steels and in particular the growth of the complex, multilayered scales observed are a direct consequence of the change in the gas composition at the end of each cycle.

KEY WORDS

Steels, ferritic, oxidation, sulfidation, cyclic

INTRODUCTION

The combustion of fossil fuels in boilers of electric power plants is presently commonly carried out in two stages. During the initial stage the air/fuel ratio is substoichiometric to decrease the NO_x emission and the associated atmospheric pollution /1,2/. This favors the formation of sulfur-containing species such as H_2S, very aggressive towards most materials even at moderately high temperatures /3-5/. The reaction is then completed by admitting an excess of air during a second stage. As a result, some plant components, and particularly the furnace waterwalls, may be exposed to gases presenting a composition changing irregularly with time from oxidizing to reducing situations and vice versa. The present research examines the effects of periodic changes in the composition of the atmospheres simulating the combustion gases on the corrosion behavior of some medium-chromium steels at 600°C considering only cycles starting with sulfidation, while those starting with oxidation will be considered elsewhere /6/.

EXPERIMENTAL

The composition of the four commercial ferritic steels used in this work, denoted as P91, NF616, 12Cr and X20, is given in Table I. Coupons of 20x10x1 mm were

machined from large pieces, polished down to 600 grit SiC paper, degreased by washing in alcohol, acetone and water and dried immediately before use. The corrosion tests were carried out at 600°C in an horizontal furnace, with samples partly immersed in silica crucibles by means of Pt suspension wires.

At the start of the test the sample tube was evacuated with a rotary pump and then filled with pure nitrogen, after which the furnace was warmed up to 600°C. After this, the reacting gas was introduced at a flow of about 3 l/hr and reached the samples after about 1/2 hr. For tests involving more than one cycle, the atmosphere was changed at the end of each cycle without intermediate cooling, to avoid extensive scale spalling. In this case the previous mixture was first displaced using a nitrogen flow for about 1/2 hr, after which a flow of the new corrosive gas was introduced.

Each cycle lasted 24 hr, while the maximum cycles number was 4. The present cycles starting with sulfidation are denoted nS, where n is the progressive cycle number. Thus, cycle 1S involves only 24 hr sulfidation, cycle 2S 24 hr sulfidation followed by 24 hr oxidation, and so on. Tests involving nS cycles were continued up to the end without intermediate weight-gain measurements.

The mixtures used initially for oxidation and sulfidation (N_2-SO_2-O_2 and H_2-H_2S-CO_2, respectively) were abandoned because the resulting kinetics were very irregular and not reproducible. The gases adopted eventually, which provided reasonably reproducible results, were an H_2-H_2S mixture and pure oxygen. The H_2S content of the H_2-H_2S mixture (1.05 vol.%) provided an equilibrium sulfur pressure of 2.4×10^{-10} atm at 600°C. The corrosion kinetics were followed by means of discontinuous weight-gain measurements carried out for each test only once at the end of the whole cycle sequence.

The corroded samples were examined by X-ray diffraction (XRD) an then mounted in resins, polished and examined by optical (OM) and scanning electron (SEM) microscopy for phase identification and microstructural analysis.

RESULTS

A - Kinetics results

The kinetics results obtained for the various cycles are shown in Fig. 1. The samples weight increases rather regularly with the corrosion time, while the four steels have a very similar behavior. A more detailed analysis of the results is obtained by comparing the effects of the various cycles. Fig. 2 shows a collective plot of the data

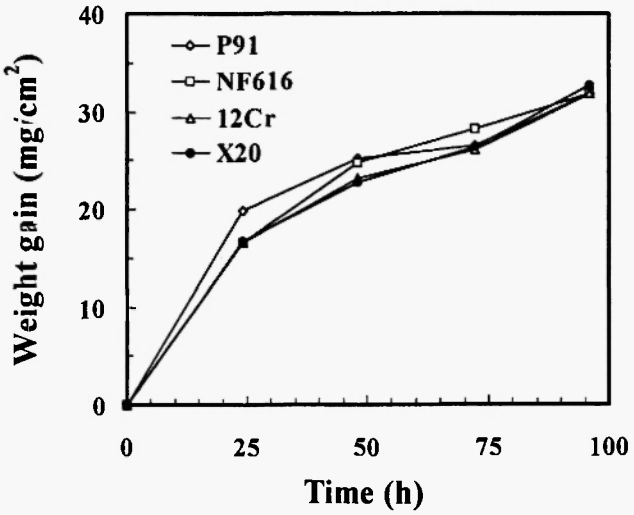

Fig. 1: Weight gains of the four steels as functions of the number of nS cycles.

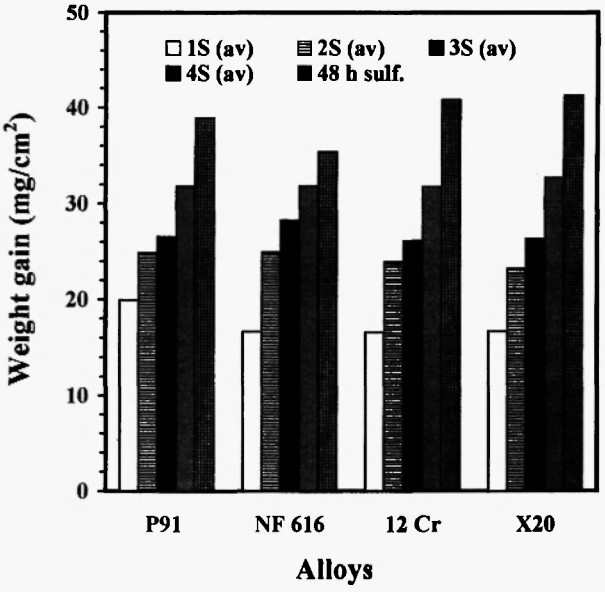

Fig. 2: Weight gains of the four steels after nS cycles and after 48 hr sulfidation (last column).

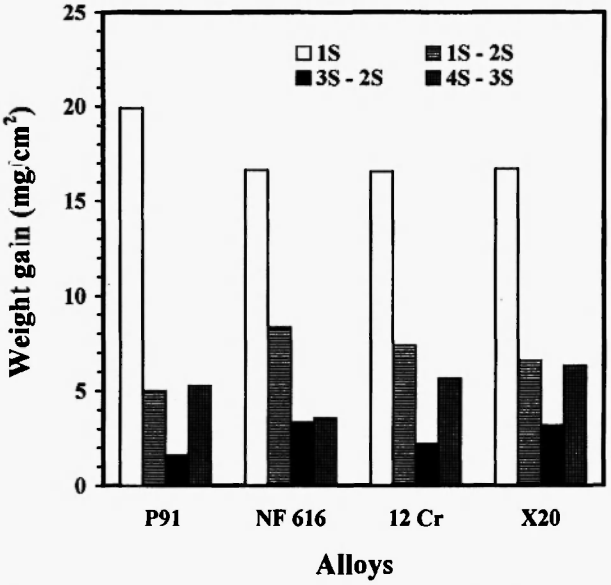

Fig. 3: Net weight gains of the four steels after each nS cycle.

obtained for the cycles from 1S to 4S for the four steels, including those measured after 48 hr of continuous sulfidation. Fig. 3 shows the differences between the weight gains measured at the end of a given cycle and those corresponding to the previous cycle, which represent the weight gains due only to the last cycle.

The weight gains due to the initial sulfidizing cycle (1S) are similar for the four steels and are also quite close to one half of those obtained after two days sulfidation, showing that the sulfidation rate of these steels is approximately linear, in agreement with the results of previous studies of the corrosion of similar steels in H_2-H_2S at 500°C /7-9/. On the contrary, those due to the second sulfidizing cycle (3S) are much lower than those due to initial sulfidizing cycle (1S), indicating the existence of a protective effect by the oxide layer formed during cycle 2S.

The weight gains due to the two oxidizing cycles (2S and 4S) are generally quite similar to each other for each steel, except for NF616 for which the weight gain due to cycle 4S is less than one half of that due to cycle 2S. In all cases the weight gains due to the oxidizing cycles are much smaller than those due to the first sulfidizing cycle (1S), but significantly higher than those due to the second sulfidizing cycle (3S) (Fig. 3).

Finally, the weight gains of the four steels due to the first oxidizing stage (cycle 2S) are much larger than those produced by the direct oxidation of the same materials for 24 hr in air without presulfidation, as reported elsewhere [6].

B - Scale structure and composition

The structure of the scales formed on the four steels after a given cycle sequence was rather similar for all materials, so that only some micrographs are used to show the general situation for each cycle.

In agreement with what has been reported previously for similar materials /7-14/, the scales formed during cycle 1S (Figs. 4-5) always contain two main layers. The outer layer is composed of large-grained, columnar FeS, generally divided into a number of rather regular

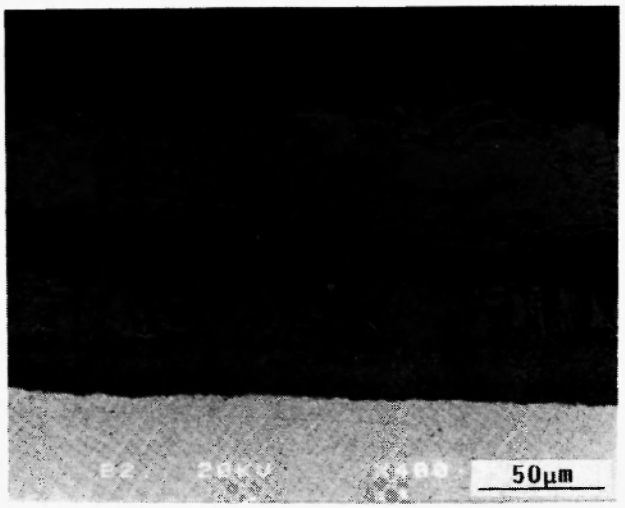

Fig. 4: Cross section of NF616 after cycle 1S (SEM).

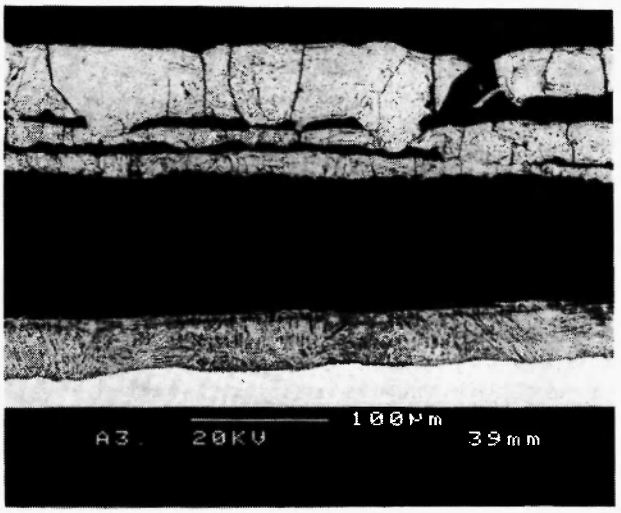

Fig. 5: Cross section of 12Cr after cycle 1S (SEM/BEI).

sublayers by a sequence of planar voids parallel to the alloy surface. On the contrary, the inner layer contains a mixture of sulfides of iron and chromium with the other impurities. In agreement with the results obtained for Fe-Cr alloys of similar composition, this layer contains a mixture of FeS, chromium sulfide and Fe-Cr thiospinel /10-14/.

The inner region of the scales formed after the first oxidizing cycle (2S) (Figs. 6-7) has essentially the same structure and composition observed after the initial sulfidizing stage. In addition, an outermost oxide layer has also grown over and in good contact with the FeS layer. According to the XRD results, this layer contains both Fe_3O_4 and Fe_2O_3.

The scales formed during the second sulfidizing cycle (3S) (Figs. 8-9) show two main types of scale structure, which occur often simultaneously on different regions of the cross section of the same sample. In the simplest case the scale contains an additional outermost sulfide layer overlying the oxide layer formed during cycle 2S and then the sulfide scale formed during the initial sulfidizing cycle (Fig. 8). In other cases, the scale contains also an additional oxide layer, thinner than the first and normally located along horizontal fissures inside the FeS layer formed during cycle 1S (Fig. 9).

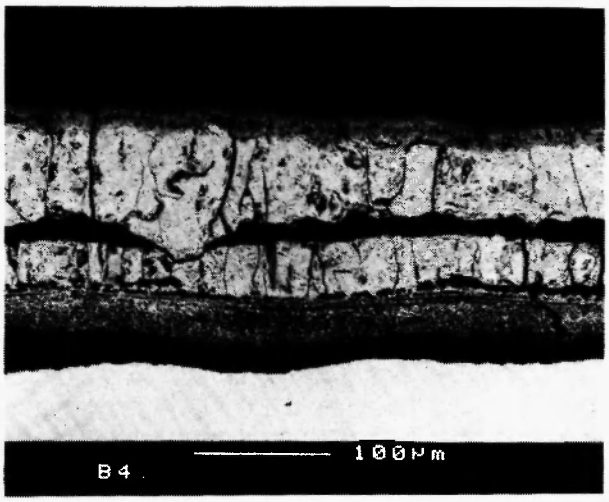

Fig. 6: Cross section of NF616 after cycle 2S (SEM/BEI).

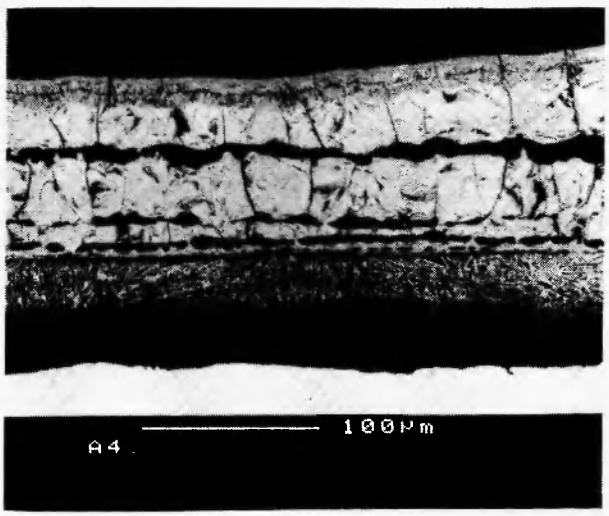

Fig. 7: Cross section of 12Cr after cycle 2S (SEM/BEI).

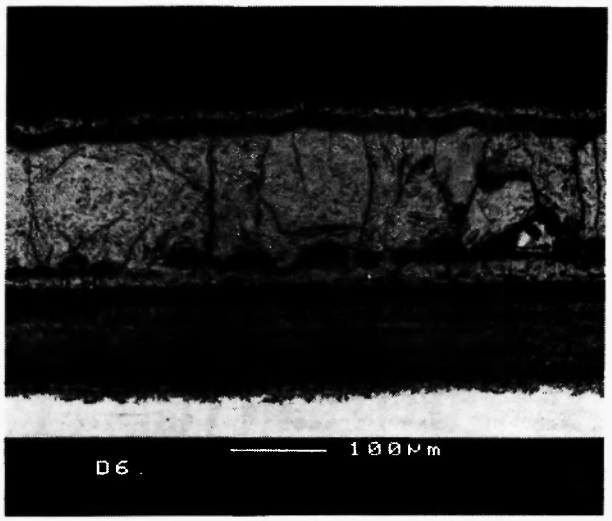

Fig. 8: Cross section of P91 after cycle 3S (SEM/BEI).

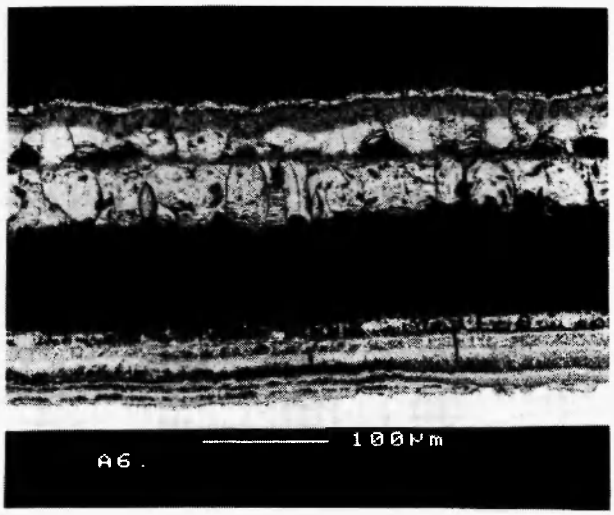

Fig. 9: Cross section of 12Cr after cycle 3S (SEM/BEI).

Finally, the scales formed during the second oxidizing cycle (4S) (Figs. 10-11) generally do not contain the sulfide layer grown during the previous cycle (3S), which should divide the oxide layers formed during the first and the second oxidizing stage (2S and 4S, respectively). The resulting structure of these scales is similar to that observed after cycle 2S, with a single external oxide layer over a single sulfide scale (Fig. 11). Sometimes these scales also contain an additional thin oxide layer inside the FeS layer (Fig. 10), as already observed at the end of cycle 3S. Moreover, the external region of the outermost oxide layer is rather porous.

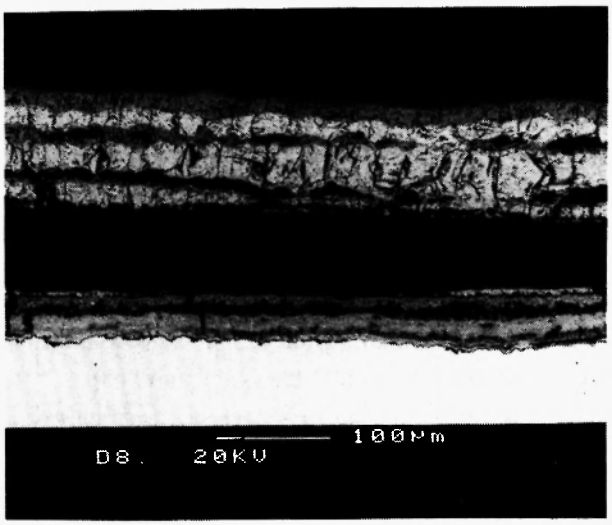

Fig. 10: Cross section of P91 after cycle 4S (SEM/BEI).

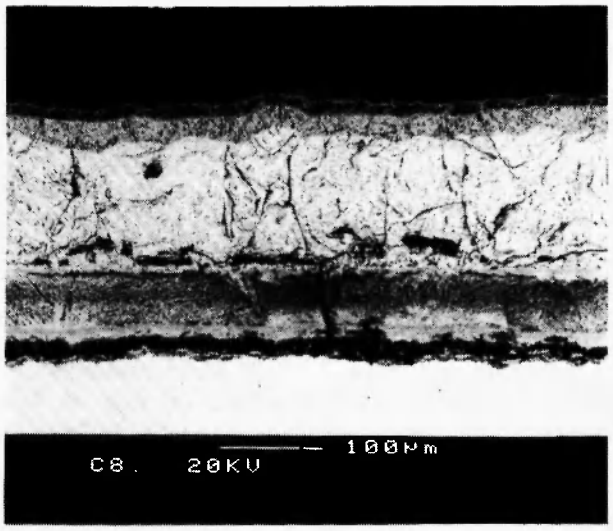

Fig. 11: Cross section of X20 after cycle 4S (SEM/BEI).

DISCUSSION

The main kinetics results of the cycles nS are 1: the rate of the second sulfidizing cycle (3S) is much lower than that of the initial sulfidation (cycle 1S); 2: the rate of the second oxidizing cycle (4S) is similar to that of the first oxidizing cycle (2S) and 3: the rate of the first oxidizing cycle (2S) is much higher than that of oxidation of the bare alloys. Moreover, FeS is not displaced from the scales when exposed to air during cycle 2S and the iron oxides are not displaced from the scales when exposed to the H_2-H_2S mixture during cycle 3S, while FeS formed during cycle 3S tends to disappear from the scales during the following cycle. The structures of the scales formed by corrosion under the present chemically cycling conditions are unusual, involving mainly the formation of alternate layers of sulfides and oxides but quite often also of irregular mixtures of the two compounds within the same layer. These kinetics and structural aspects are strictly interconnected, as examined below.

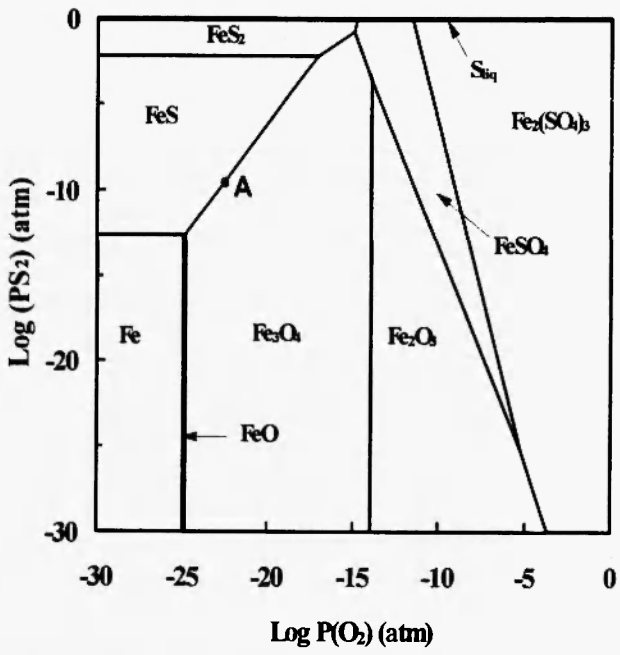

Fig. 12: Isothermal phase diagram of the ternary Fe-O-S system at 600°C.

For simplicity, the following qualitative analysis considers only the behavior of pure iron, which is the main component of the steels examined. In agreement with a study of the effect of a preoxidation on the subsequent sulfidation of pure iron by Rahmel and Gonzalez /15/, it is also assumed as an approximation that the various layers are compact and that the oxide and the sulfide do not react at their interface and do not dissolve into each other.

According to the isothermal phase diagram for the ternary Fe-O-S system at 600°C (Fig. 8) FeS is absolutely unstable when exposed to oxygen at the reaction temperature. Thus, the sulfide grown during cycle 1S should decompose and transform into oxide when exposed to oxygen during cycle 2S. However, this reaction is hindered by the rapid growth of the new oxide layer over FeS, which prevents a direct contact between the reactants: in this condition FeS can survive beneath the oxide layer, even though in a metastable state. The same situation applies when an oxide layer is exposed to the H_2-H_2S mixture where it is unstable. Thus, the scales obtained in this study are generally composed of a sequence of alternate sulfide and oxide layers.

During each cycle the iron activity in the scale, a(Fe), must decrease regularly from the alloy/scale to the scale/gas interface to provide the outward metal flux required for the reaction with the gas phase. However, the behavior of the pressures of the two oxidants across the scale is more complex. In fact, the sulfur pressure inside a sulfide layer simply is related to the local iron activity by

$$a(Fe) = [K(FeS)\, P(S_2)]^{-1/2}$$

where K(FeS) is the equilibrium constant for the formation of FeS. Similarly, the oxygen pressure inside a layer of an oxide Fe_aO_b is related to the local iron activity by

$$a(Fe) = [K(Fe_aO_b)\, P(O_2)^{b/2}]^{-1/a}$$

where $K(Fe_aO_b)$ is the constant of equilibrium for the formation of Fe_aO_b. On the contrary, the pressure of sulfur inside an oxide layer and that of oxygen inside a sulfide layer drop essentially to zero, producing non-equilibrium conditions between the various layers.

The iron activity in FeS in equilibrium with the sulfur pressure of the present H_2-H_2S mixture, a(Fe,1), is equal to 0.0154 and falls in the field of stability of FeS, while that in equilibrium with 1 atm O_2, a(Fe,2), is equal to 1.7×10^{-18} and is within the range of stability of Fe_2O_3. These a(Fe) values are those prevailing at the scale surface during the sulfidizing and oxidizing stages, respectively, if this is in equilibrium with the gas. Moreover, the oxygen pressure in equilibrium with a(Fe,1) is equal to 7.2×10^{-23}, which falls in the field of stability of Fe_3O_4, while that of sulfur in equilibrium with a(Fe,2) is above the vapor pressure of liquid sulfur at 600°C, and thus is not even attainable.

Under overall equilibrium conditions the iron activity at the scale/gas interface during cycle 2S is equal to a(Fe,2), while that at the sulfide/oxide interface must be the same in the two compounds. As long as the sulfur pressure at this site remains equal to that prevailing during cycle 1S, the local a(Fe) must correspond to the FeS-Fe_3O_4 equilibrium and thus is represented by a single point along the line for the FeS-Fe_3O_4 equilibrium (point A in Fig. 8).

The actual situation prevailing during cycle 2S may differ even considerably from the previous equilibrium condition. In fact, when the steels are exposed to oxygen at the end of the first stage, the iron activity at the outer scale surface must decrease from a(Fe,1) down to a(Fe,2). Moreover, the iron activity in the oxide at its interface with FeS must be higher than a(Fe,2), but at the same time also lower than a(Fe,1), to provide an appropriate profile of a(Fe) through the external oxide layer. Thus, the kinetics of oxidation will depend simultaneously on the thickness of both the sulfide and oxide layers and on their transport properties, which are affected by the conditions established at their interfaces.

More specifically, the metal fluxes through the two layers are given by [16]

$$J_M(FeS) = c°(FeS)\, k_x(FeS)/2X(FeS)$$

and

$$J_M(FeO_x) = c°(FeO_x)\, k_x(FeO_x)/2X(FeO_x)$$

where c°(i) is the concentration of iron in the corresponding compound (moles cm^{-3}), X(i) the thickness of the i layer at time t and $k_x(i)$ the corresponding parabolic rate constant in terms of scale thickness. These rate constants depend on the oxidant pressures prevailing at the inner and outer interfaces of

each single layer /16/ and thus will in general be functions of time when the corresponding pressures evolve during the reaction.

In the absence of reactions between FeS and the iron oxides, as assumed here, the flux of iron through the outer oxide and the inner sulfide layers must be the same. Moreover, the thickness of the inner sulfide layer during cycle 2S is constant, while $k_x(FeS)$ may change as a result of a change of $P(S_2)$ at the sulfide/oxide interface. Similarly, the overall parabolic rate constant for the growth of the external oxide layer, which is in general a combination of those for the growth of the various iron oxides /17/, will also change as a result of the evolution of $P(O_2)$ at the inner interface of the oxide layer. Finally, the iron flux through the oxide layer will also depend on the oxide thickness, which increases with time.

Since the fluxes of iron through the sulfide and oxide layers must be identical, at the beginning of cycle 2S the rate constant $k_x(FeO_x)$ will be very small to produce a finite iron flux in spite of the very small thickness of the oxide layer. If the scale/gas interface is at equilibrium, the iron activity in the oxide at the sulfide/oxide interface [a(Fe,ox,int)] must be quite close to a(Fe,2) and thus much smaller than a(Fe,1), implying a lack of local equilibrium, as assumed by Rahmel and Gonzalez /15/. At the same time, the iron activity inside the sulfide at this site may remain initially equal to a(Fe,1), producing a constant iron flux through FeS, resulting thus in linear overall corrosion kinetics [15]. To maintain a constant rate of oxide growth in spite of the linear increase of $X(FeO_x)$, $k_x(FeO_x)$ must also increase linearly with time, involving a simultaneous decrease of a(Fe,ox,int).

With time a(Fe,ox,int) must approach gradually a(Fe,1), so that a linear increase of $k_x(FeO_x)$ will no longer be possible. At this point the corrosion rate will begin to decrease, due to the increase of the oxide thickness. At the same time, the iron flux through FeS must also decrease, implying a decrease of $k_x(FeS)$ which occurs through an increase of a(Fe,sulf,ext). In this way, the iron activities inside FeS and inside the iron oxide at their interface will become eventually equal to each other.

After reaching the equilibrium, the iron activity at the sulfide/oxide interface will continue to increase with time to reduce further the overall scaling rate, implying a simultaneous decrease of the corresponding oxygen and sulfur pressures. In particular, when the local oxygen pressure decreases below the $FeO\text{-}Fe_3O_4$ equilibrium, FeO will start to appear beneath the Fe_3O_4 layer. Finally, when the oxygen pressure at the sulfide/oxide interface approaches sufficiently the value for the Fe/FeO equilibrium, $k_x(FeO_x)$ will become practically constant and the overall rate will become practically parabolic. In fact, both FeO and Fe_3O_4 are p-type oxides and thus are not very sensitive to the oxygen pressure prevailing at their inner interfaces /16/. Thus, in the most general case the rate is expected to undergo a gradual change from a linear to a parabolic behavior. A kinetics behavior of this type has been reported by Rahmel and Gonzalez for the oxidation of iron followed by sulfidation /15/. A detailed quantitative analysis of the kinetics of the oxidation-sulfidation of iron for a sequence of two cycles will be presented elsewhere [18].

The rate of oxidation of the present steels during cycle 2S is much higher than that of oxidation of the bare alloys at the same temperature, as reported elsewhere /6/. The main reason for this is that direct oxidation of these alloys produces rather protective scales containing chromia or mixtures of chromia with Fe-Cr spinel $(Fe,Cr)_3O_4$ /16/. On the contrary, oxidation of the same steels after sulfidation produces only pure iron oxide scales because the impurities such as chromium are confined inside the innermost region of the initial sulfide layer. At the same time a rather large iron flux is provided to the growing oxide by diffusion of iron through the non-protective inner sulfide layer.

The situation existing during the second sulfidizing stage (cycle 3S) is similar, but more complex. In fact, at the beginning of cycle 3S the iron activity at the surface of the oxide layer formed during cycle 2S must increase from a(Fe,1) to a(Fe,2) with a simultaneous decrease of the oxygen activity at the surface of the same layer. Since a(Fe,1) is within the range of stability of Fe_3O_4, the external Fe_2O_3 layer must be initially reduced to Fe_3O_4. During cycle 3S the oxide layer grown during cycle 2S is sandwiched between two sulfide layers and exposed to a very small drop of oxygen activity, while its thickness remains approximately constant. Thus, the

maximum iron flux which can diffuse through this intermediate oxide layer must be small and will control the sulfidation rate during this stage, which is thus much slower than during the cycle IS. At the same time, the flux of iron across the innermost sulfide layer must also decrease with respect to cycle 2S. For this, the sulfur pressure at the interface between the innermost sulfide and the oxide layer must decrease, producing a corresponding reduction of k_x(FeS) for this layer.

The oxidation rate during cycle 4S is approximately the same as during cycle 2S, but larger than that of sulfidation during cycle 3S. At the beginning of this cycle the iron activity at the scale surface must decrease again, tending to a(Fe,2). If the scale were formed by a sequence of two sulfide and two oxide alternate layers, the corrosion rate would be controlled again by the slow transport across the intermediate oxide layer as during cycle 3S. However, the sulfide layer formed during the second sulfidizing stage (cycle 3S) tends to disappear during cycle 4S, so that the scale structure becomes equivalent to that observed during cycle 2S, with a large drop of iron activity through a single external oxide layer overlying an inner sulfide layer. Thus, the iron flux through the oxide layer can again be rather large, even if smaller than during cycle 2S due to the increased oxide thickness. The disappearance of the second sulfide layer may occur either by loss of sulfur in the gas, as suggested by the extensive porosity of the outermost scale layer, or by migration of sulfur inwards to form new sulfide in the inner scale region.

A peculiar feature of these scales is the formation of oxide within the sulfide layers and of sulfide inside the oxide layers and in particular of an oxide layer inside the initial sulfide layer during cycle 2S. As examined above, the conditions existing during a given cycle are favorable to the penetration of the last oxidant inside the underlying layer of the compound of the previous oxidant, where its activity is probably close to zero. This process is normally prevented by the very low solubility and diffusivity of oxygen in FeS and of sulfur in iron oxides. However, if the layer grown during the previous cycle contains cracks or fissures, the last oxidant can penetrate inwards by means of gas-phase transport and form the corresponding compound locally. Similar processes may occur during any stages after the first and result in the final growth of the complex mixtures of oxides and sulfides observed experimentally.

CONCLUSIONS

The corrosion of medium-chromium steels at 600°C in gases whose composition changes cyclically with time from sulfidizing to oxidizing conditions and vice versa produces complex scales, essentially composed of alternate sulfide and oxide layers. In fact, each cycle produces a new layer containing a compound of the relevant oxidant overlying those formed during the previous cycles, which are generally able to survive even under unfavorable thermodynamic conditions. However, penetration of each oxidant through the underlying layer of the other oxidant, mainly occurring through discontinuities of the scales, also produces irregular mixtures of the two compounds in the various scale regions.

The rates of oxidation of the steels during the second cycle are significantly accelerated by the initial sulfidizing stage with respect to those of direct oxidation of the same alloys. This deleterious effect is due to the presence of a sulfide layer in contact with the alloy, which remains stable during the subsequent oxidizing cycle, through which iron can diffuse much more rapidly than through the rather protective scales formed by direct oxidation of the steels. Further exposure of the duplex sulfide-oxide scales to the two kinds of gases produces lower weight gains. The overall scaling kinetics are controlled by the nature and thickness of the various layers, by their sequence and by the profiles of iron activity through each of them and through the whole scale, which change from cycle to cycle.

ACKNOWLEDGMENTS

The support of this work by the European Community through Contract N. CHRX-CT94-0519 is gratefully acknowledged. One of us (C. Roos) is also grateful to the European Community for a grant used to carry out the present research.

REFERENCES

1. S.F. Chou, P.L. Daniel, A.J. Blazewicz and R.F. Dudek, in: *High Temperature Corrosion in Energy Systems*, M.F. Rothman (Ed)., The Met. Soc. of AIME, Warrendale, 1985, p. 327.
2. P.L.Daniel, J.D. Gottshling and A.S. Miller, in: *Corrosion-Erosion-Wear of Materials in Emerging Fossil Energy Systems*, A.V. Levy (Ed.), NACE, Houston, 1982, p. 137.
3. S. Mrowec and K. Przybylski, *High Temp. Mater. and Proc.*, **6**, 1 (1984).
4. D.B. Meadowcroft, *Mater. Sci. and Engin.*, **A121**, 669 (1989).
5. F. Gesmundo, D.J. Young and S.K. Roy, *High Temp. Mater. and Proc.*, **8**, 149 (1989).
6. C. Roos, D. Oquab and F. Gesmundo, to be published.
7. F. Gesmundo, W. Znamirowski, F. Viani and F. Bregani, *Proc. International Symposium on High-Temperature Corrosion*, H. Guan, W. Wu, J. Shen and T. Li Eds., Liaoning Science and Technology Publ. House, Shenyang (China), 1991, p. 139.
8. F. Gesmundo, K. Godlewski, F. Viani and F. Bregani, *Bull. Polish Acad. Sci., Chemistry*, **40**, 1 (1992).
9. F. Gesmundo, F.Viani, W. Znamirowski, K. Godlewski and F. Bregani, *Werkst. und Korros.*, **43**, 83 (1992).
10. T. Narita and K. Nishida, *Oxid. Met.*, **6**, 157 (1973)
11. T. Narita and K. Nishida, *Oxid. Met.*, **6**, 181 (1973)
12. P.D. Zelanko and G. Simkovic, *Oxid. Met.*, **8**, 343 (1974).
13. D.J. Young, *Rev. on High Temp. Mater.*, **4**, 299 (1980).
14. T. Narita, W.W. Smeltzer and K. Nishida, *Oxid. Met.*, **17**, 299 (1982).
15. A. Rahmel and J.A. Gonzalez, *Werkst. und Korros.*, **13**, 433 (1973).
16. P. Kofstad, *High Temperature Corrosion*, Elsevier Applied Science, New York, 1988.
17. F. Gesmundo and F. Viani, *Corros. Sci.*, **20**, 541 (1980).
18. F. Gesmundo *et al.*, to be published.